Chemical Engineering Journal 294 (2016) 323–332

Contents lists available at ScienceDirect

Chemical Engineering Journal

journal homepage: www.elsevier.com/locate/cej

Insecticide as a precursor to prepare highly bright carbon dots for patterns printing and bioimaging: A new pathway for making poison profitable

Wen-Sheng Zou [a,b,*], Ya-Jun Ji [a], Xiu-Fang Wang [a], Qing-Chun Zhao [a], Jun Zhang [a], Qun Shao [a], Jin Liu [a], Feng Wang [a], Ya-Qin Wang [a,*]

[a] Anhui Key Laboratory of Advanced Building Materials and Key Laboratory of Functional Molecule Design and Interface Process, Anhui Jianzhu University, 856 South Jinzhai Road, Hefei, Anhui 230022, China
[b] Institute of Intelligent Machines, Chinese Academy of Sciences, Hefei, Anhui 230031, China

HIGHLIGHTS

- Insecticide as a precursor was used to prepare highly bright C-dots.
- Solvent- and temperature-dependent synthesis was investigated.
- Lab-leveled mimetic insecticide residual was attempted to synthesize C-dot.
- The insecticide-based C-dots were used in printing patterns and bioimaging.

GRAPHICAL ABSTRACT

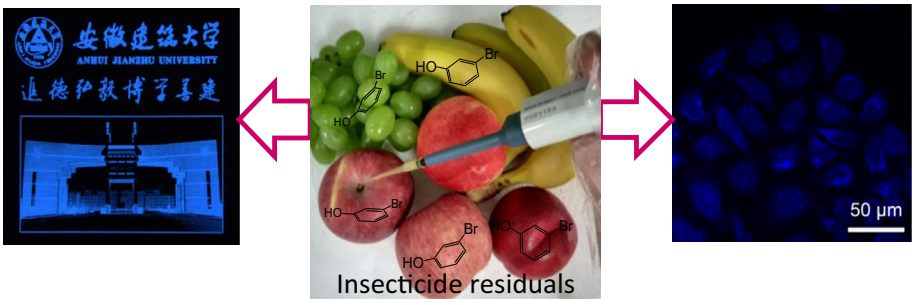

ARTICLE INFO

Article history:
Received 10 December 2015
Received in revised form 27 February 2016
Accepted 1 March 2016
Available online 4 March 2016

Keywords:
3-Bromophenol
Insecticide residuals
Carbon dots
Patterns printing
Bioimaging

ABSTRACT

Halophenols (HPs) inflict adverse impacts on human and environment due to their toxic, carcinogenic as well as teratogenic properties. Additionally, it is of great importance and urgency for the development of simple, efficient and inexpensive approaches to minimize the harm of HPs. Here we report an innovatively making poison profitable method to prepare carbon dots (C-dots) using 3-bromophenol residual as a precursor. The effects of solvent and carbonization temperature on the preparation of insecticide-based C-dots were investigated. The results indicate that higher organic solvent content in solution and higher carbonization temperature are in favor of the formation of C-dots with smaller size and higher quantum yields. Meanwhile, all C-dots displayed excellent water solubility and high photostability against ionic strengths and light illumination. The possible mechanisms of polymerization and carbonization of C-dots were rationally proposed, and the incompact framework structure of C-dots was reasonably inferred by room-temperature phosphorescence measurement. Also, a kind of low toxicity, good biocompatibility and photostability C-dots, which were synthesized *via* a lab-leveled mimetic insecticide residuals approach, were utilized as colorless inks for printing patterns and as fluorescence probe for bioimaging. This proposed approach opened up a potential prospect to efficiently utilize pesticide residuals and other hazardous chemicals for biolabeling and bioimaging.

* Corresponding authors at: Anhui Key Laboratory of Advanced Building Materials and Key Laboratory of Functional Molecule Design and Interface Process, Anhui Jianzhu University, 856 South Jinzhai Road, Hefei, Anhui 230022, China (W.-S. Zou).
E-mail addresses: wszou@ahjzu.edu.cn (W.-S. Zou), yqwang@ahjzu.edu.cn (Y.-Q. Wang).

http://dx.doi.org/10.1016/j.cej.2016.03.004
1385-8947/

1. Introduction

More and more research interest has grown in the fields of fluorescent carbon-based nanomaterials, that is carbon quantum dots (C-dots), due to their exciting advantages such as high chemical inertness, outstanding photostability, excellent water solubility, ease of synthesis and modification, low toxicity and good biocompatibility [1–6], which makes these nanomaterials promising alternatives to metal-based quantum dots (QDs) with high toxicity for biosensing, bioimaging, drug and gene delivery, as well as other biological related aspects [7–9]. Besides, it was found that C-dots exhibits strong fluorescence upon two photo excitation in the near infrared region, which further broadened their applications in bioimaging [10,11]. Also, heteroatoms doped carbon nanomaterials are considered as the most promising and suitable candidates to complement carbon in materials applications because of their tunable electronic properties as well as their surface and local chemical reactivities [12,13]. Considerable attentions have been therefore focused on incorporating heteroatoms other than N, whether alone or with other dopants, into C-dots to modulate their intrinsic properties [14–16].

Different from the synthesis of metal-based QDs and upconversion nanoparticles, the high purity chemicals must be required and the few rare-earth elements are limited to use. Whereas the raw materials for C-dots are nearly hands-down. Several published papers have reported the preparation of fluorescent C-dots using natural precursors such as hair fiber [17], humic substances [18], carbon black [19], milk [20], glycine [21], carbohydrates [10,22,23], resol [24], glycerol [25], candle soot [26], fruits [27–29], and so on, which are widely distributed in any corner of nature and our daily life, and easily available to replace traditional chemicals reagents. These synthesized C-dots integrate advantages of high brightness, low cost and multicolorful emission as well as above mentioned ones. In consideration of the varieties of goods of C-dots, it is naturally expected much more materials, even including pesticides with high toxicity, to be potential precursors for synthesizing advanced fluorescent carbon nanomaterials. To the best of our knowledge, there has still no reports on the synthesis of C-dots using pesticide as a precursor.

Halophenols (HPs) are a group of pollutants that are incorporated into the environment largely due to industrial activities, which are widely used as chemical intermediates, fungicide, insecticide and herbicide [30,31], and frequently used in the wood industry to control fungi and as a flame retardant [32,33]. Due to their constant use, these compounds become common pollutants of soils, freshwater and environmental organisms. Therefore, HPs inflicted adverse impacts on the ecosystem for their toxic, carcinogenic and teratogenic properties. It was suspected that HPs disrupted the humoral system by either showing thyroid hormone like activity [34] or binding to the human estrogen receptor [35]. The reported works have revealed that HPs compounds exerted their toxic effect on membrane mainly by acting as uncoupling agents [36–38]. In recent years, more and more concerns have been emerged owing to their persistence and bioaccumulation in both animals and humans [39,40]. Therefore, it is of great importance to find innovative and effective approaches to minimize the harm of HPs in environment and ecology.

Herein a facile and low-cost strategy is developed for the synthesis of highly bright C-dots using an insecticide, 3-bromophenol (3-BP), as a precursor. The effects of temperature, solvent and pH on emission properties of the as-prepared insecticide-based C-dots were investigated. The results indicate that both much higher carbonized temperature and much thicker organic solvent are in favor of the formation of C-dots featuring monodispersion, high yield and smaller size. The brightly blue fluorescence of the C-dots at ~450 nm was observed in both solid state and liquid one. Whereas the room-temperature phosphorescence (RTP) at 528 nm with 3.7 ms of decay time was observed in solid state but disappeared in solution, revealing the incompact framework structure of the C-dots. Moreover, the prepared C-dots were also applied in patterns printing and bioimaging, exhibiting the excellent photostability, low toxicity, good biocompatibility and high water solubility of insecticide-based C-dots. Due to simplicity and effectivity, this proposed approach opened up a promising gate for efficient utilization of insecticide residuals.

2. Materials and methods

2.1. Materials

3-BP (purity over 99%) was the product of Alfa Aesar (Tianjin, China). All other reagents were of analytical grade and commercially purchased from Sinopharm Chemical Reagent Co., Ltd. (Shanghai, China), and used without further purification.

2.2. Characterizations

The RTP, fluorescence spectra and lifetime evaluation of RTP were recorded on an F-4600 (Hitachi, Tokyo, Japan), and the measurements were performed with different excitation wavelength equipped with a plotter unit and a quartz cell (1 × 1 cm) in a variety of modes. UV–vis absorption spectra were obtained using a Shimadzu 3100 UV–vis spectrophotometer. Scanning electron microscopy (SEM) images of the product were taken on a field emission scanning electron microscope (FESEM, JEOL, JSM 7500F). The X-ray photoelectron spectroscopy (XPS) was performed with an XPS instrument (ThermoESCALAB250, USA) using Al Ka X-ray source (1486.6 eV). Fourier transform infrared (FT-IR) spectra (4000–400 cm^1) in KBr were recorded on a Nicolet-6700 spectrometer (Nicolet, Madison, WI, USA). The morphology of the colloidal particles were characterized by transmission electron microscopy (TEM) on a JEM-200CX (JEOL, Tokyo, Japan) microscope operating at a 200 kV accelerating voltage. The powder X-ray diffraction (XRD) spectra were collected on a Shimadzu XRD-6000 diffractometer with Cu Kα radiation. The acidity was measured with a Sartorius PB-10 pH meter (Sartorius, Dietikon, Switzerland). The fluorescence lifetime measurements were recorded on an Edinburgh Analytical Instruments F900 using hydrogen lamp as a light source and 365 nm as an excitation wavelength. Decay curve for C-dots was monitored at 450 nm. The solutions containing C-dots were analyzed for ξ-potential values using dynamic light scattering (Nano-Z, Malvern, UK) with laser wavelength at 633 nm and a measurement angle of 173° (backscatter detection) at 25 °C.

2.3. Quantum yields (QY) measurements

Quinine sulfate (0.1 M H_2SO_4 as solvent; QY = 0.54) was selected as a reference. The QYs of C-dots (in water) were calculated by slope method using the reference of quinine sulfate: compared the integrated photoluminescence intensity and the absorbance value of the samples with that of the references [41]. The φ_x was calculated according to following Eq. (1):

$$\varphi_x = \varphi_{st}(K_x/K_{st})(\eta_x/\eta_{st})^2 \quad (1)$$

where φ is the QY, K is the gradient from the plot of integrated fluorescence intensity *versus* absorbance, and η is the refractive index of the solvent; ST and x denote the standard and the sample, respectively. For the aqueous solutions, the η_x/η_{st} value is equal to 1.

2.4. Synthesis of insecticide-based C-dots

The C-dots were prepared by referring to a previous report [42]. Briefly, 0.2 g of 3-bromophenol (3-BP) was dissolved in 20 mL of different mixed solvent. The solution was bubbled with N_2 for 1 h to exclude dissolved oxygen, and then transferred to the Teflon-lined autoclave and heated to different temperature for 8 h. After naturally cooling to room temperature, the as-prepared C-dots was centrifuged at 10,000 rpm for 10 min to remove large precipitates. For further purifying the C-dots, the original solution was concentrated by rotary evaporation at 60 °C. After that, the concentrated C-dots were re-dispersed in mixed solution of 2:1 (v/v) water and dichloromethane for 3 times to remove the unreacted 3-BP molecules. The purified C-dots were preserved in refrigerator at 4 °C for further use.

2.5. Insecticide-based C-dots as ink for patterns printing

The purified C-dots were diluted into water to form solution with given concentration. The colorless C-dots aqueous solution was poured into a vacant cartridge from a commercial inkjet printer. A commercially available filter paper with no background UV fluorescence on which the C-dots adhered well was chosen as the printing paper. The Logo and Chinese/English names of Anhui Jianzhu University were printed on the filter paper by the inkjet printer after the treatment of dryness. The photographs were taken with a canon 350D digital camera under a 365 nm UV lamp.

2.6. Cellular toxicity test

The cytotoxicity study of as-prepared insecticide-based C-dots was conducted using the MTT assay on HeLa cells. The MTT assay was carried out according to previous report [43]. Briefly, HeLa cells were seeded in 96-well plates at 1×10^4 cells per well in Dulbecco's Modified Eagle's Medium (DMEM) medium with 10% fetal bovine serum and 100 μg/mL penicillin/streptomycin and maintained at 37 °C, 95% relative humidity and 5% CO_2. After incubating for 24 h, the medium was replaced with 100 μL of fresh medium containing a concentration of C-dots (from 0 to 100 μg mL^{-1}). At certain appropriate time interval (24 h or 48 h), the medium was removed, followed by adding fresh medium (100 μL) containing MTT (20 μL, 5 mg mL^{-1}) into each well. After incubating the cells for another 4 h, the absorbance of the solution was measured to assess the relative viabilities of the cells by a Bio-Rad 680 microplate reader. Optical density (OD) was read at a wavelength of 490 nm. The cell viability was estimated according to the following Eq. (2)

$$\text{Cell viability} = \text{OD}_{\text{Treated}}/\text{OD}_{\text{Control}} \times 100\% \quad (2)$$

where $\text{OD}_{\text{Control}}$ and $\text{OD}_{\text{Treated}}$ are the optical density in the absence and in the presence of C-dots, respectively.

2.7. Cellular imaging

HeLa cells (1×10^4) were plated in a cover-glass-bottom dish in DMEM supplemented with 10% fetal bovine serum and 100 μg mL^{-1} penicillin/streptomycin. After incubating for 24 h, the cells were incubated with 100 μg mL^{-1} C-dots for 4 h. The cells were then washed with phosphate buffered salt (PBS) for three times to remove the excess C-dots. The images were immediately taken by a confocal laser scanning microscope after the incubation and washing operations.

3. Results and discussion

3.1. Preparation and characterization of insecticide-based C-dots

HPs are present in marine organisms and are thought to cause the typical sea-like taste and flavor, which may play a role in chemical defense and deterrence [33]. However, due to constant use in chemical and wood industries, HPs have been detected in soils, water and environmental organisms. The photocatalytic degradation is the currently useful method for the treatment of phenolic compounds, which has, however, always been persecuting by time-consuming, cost-ineffective and mineralization-incomplete catalytic procedure [40,44]. Recently, with rapid developments in C-dots research, the functionalization of C-dots and their applications, especially in bioimaging have become a hotspot [45,46]. On the other hand, the precursors of the C-dots are not limited in conventional chemical reagents with high purity and the reaction condition is relatively simple [16–29]. Both of which, together with few reported aromatic compounds containing-based C-dots [42,47], inspired us to reason that HPs may be carbonized at appropriate solvothermal condition in pursuit of highly bright C-dots.

3.1.1. Effect of solvent on preparation and characterization of insecticide-based C-dots carbonized at 170 °C

Using 3-bromophenol (3-BP), representative of HPs, as a precursor was adopted to synthesize C-dots. For seeking green synthesis approach and utmost decreasing the amount of organic solvent, the effect of solvent on preparation of C-dots at 170 °C, that is the mixed solvent of ethanol and water with ratio of (v/v) 1:9, 3:7, 5:5, 7:3 and 9:1, were attempted. Briefly, 0.2 g of 3-BP was completely dissolved in ethanol, followed by addition of different amount of water and ethanol to obtain solutions with above ratio solvent. The resulting solutions were transferred to the Teflon-lined autoclave and heated to 170 °C for 8 h after the exclusion of dissolved oxygen. The different C-dots, correspondingly denoted as 1#, 2#, 3#, 4# and 5#, were obtained *via* centrifuging for one time and then purification for several times. Due to the solubility of 3-BP became well and well in above solution, the outputs of C-dots also gradually increased. In consideration of the relatively high quantum yield (19.6%, quinine sulfate as a reference, *vide post*) and high output (without precipitation) of 5# C-dots, the XPS, TEM, FTIR, XRD, lifetime decay, etc. were performed to characterize 5# C-dots.

XPS was employed to provide convincing evidences for the surface state of C-dots. The XPS spectrum of C-dots shown in Fig. 1A exhibits the as-prepared C-dots is composed of carbon, oxygen, and bromine. The obvious C and Br peaks were detected with binding energy at around 285 eV, and 183.7 and 69.7 eV, respectively. In the high-resolution C1s XPS spectrum of the insecticide-based C-dots (Fig. 1B), three peaks are observed with the binding energies of about 284.5, 286.7 and 288.5 eV, which are attributed to C—O/COOR, aromatic C—Br, and C—C/C=O species, respectively [16]. The high-resolution Br3d XPS spectrum in Fig. 1C has two peaks at 70.4 and 68.6 eV, which are attributed to the aromatic C—Br, and bromine anion, respectively [48]. SEM images of C-dots gave the same result as XPS (see Fig. S1). Also, FTIR spectrum of the C-dots (see Fig. 2A) shows the presence of the same groups. The peak at 1027 cm^{-1} is ascribed to alkoxy C—OH stretching vibration [49]. The peak at 1595 and 1231 cm^{-1} are assigned to the aromatic C=C and epoxide/ether C—O—C, respectively [50]. The peak from 1390 to 1490 cm^{-1} can be identified as COO^- group [21]. A small band at 2916 cm^{-1} is the C—H bonds. The peak at 1650 cm^{-1} is ascribed to the C—O stretching vibration [19]. The peak at 675 cm^{-1} is attributed to aromatic C—Br bonds. In addition, the broad peak around 3425 cm^{-1} occurs at FTIR curve because of O—H bonds.

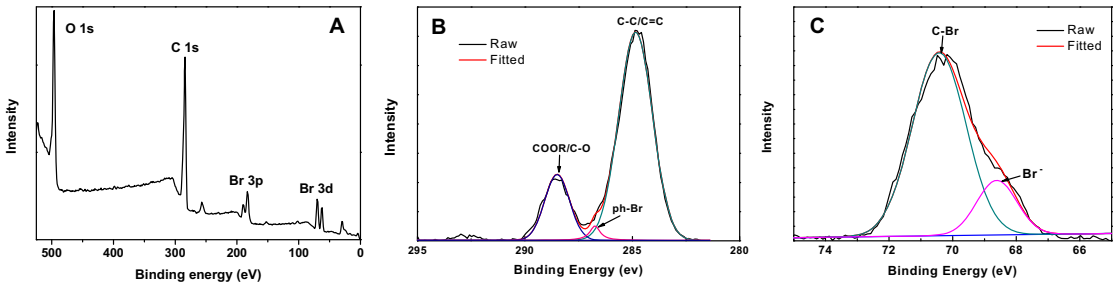

Fig. 1. XPS spectra of C-dots (A). High-resolution XPS data of C1s (B) and Br3d (C) of C-dots.

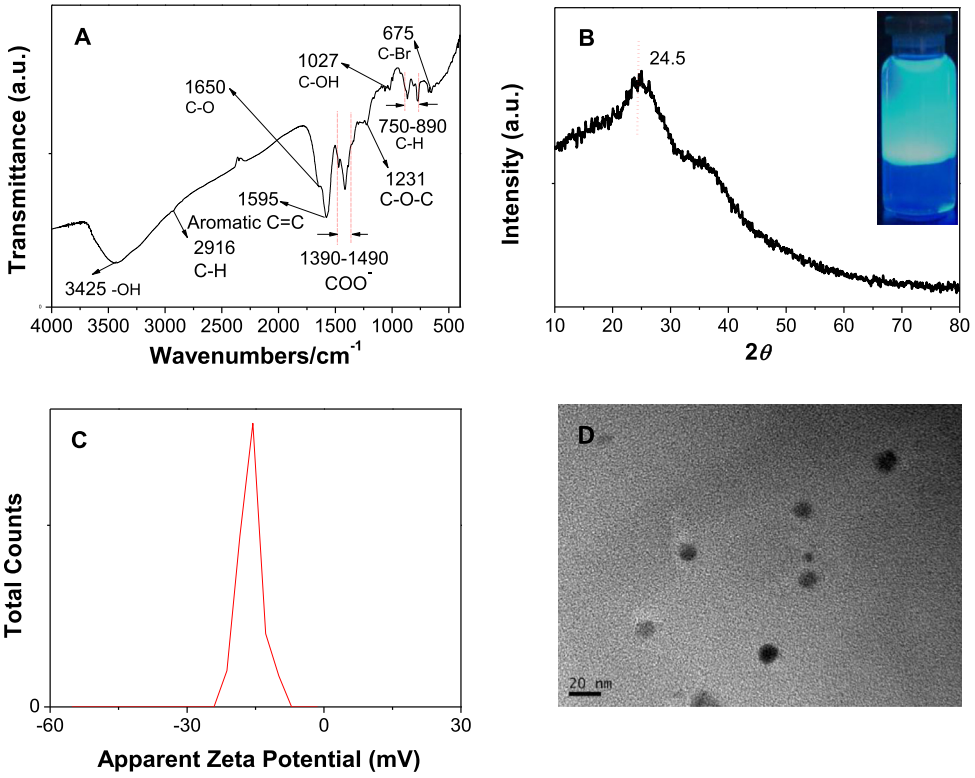

Fig. 2. FTIR spectrum (A), XRD pattern (B), zeta potential (C) and TEM image of C-dots (D). The inset in B is the image of C-dots was dispersed in mixed solvent of water and dichloromethane.

The band ranging from 750 to 890 cm^{-1} is the C—H bending vibration. The XRD pattern of the C-dots shown in Fig. 2B displays a broad peak at about 24.5°, revealing an amorphous carbon phase, which is possibly, attributed to the introduction of C—O—C, COOR etc. groups. When the C-dots was dispersed in the mixed solvent of water and dichloromethane, the water layer displayed high brightness, but dichloromethane one, colorlessness, suggesting the excellent water solubility of C-dots (see inset in Fig. 2B).

As shown in Fig. 2C, the zeta potential of the C-dots was detected as −15.8 mV, suggesting C-dots are negatively charged due to large amount of hydroxyl and a little carboxylic groups anchoring on the surface of the C-dots (see Fig. 5, *vide post*). Meanwhile, these functional groups on the surface may bring in a series of emissive traps, which are of great importance for the strong photoluminescent property exhibited by the C-dots [29]. The TEM image in Fig. 2D shows small particle size in a relatively narrow size distribution and monodispersion of C-dots. The statistical particle size distribution of the C-dots is 2.5–6.5 nm with average diameter 5.2 nm. However, HRTEM image of the C-dots do not reveal any clear lattice fringe, indicating its amorphous nature, which coincides well with the XRD result.

3.1.2. Emission properties of insecticide-based C-dots

To explore the optical properties of the C-dots, the photoluminescence and UV–vis absorption spectra were studied at room temperature, and the normalized spectra of 1# to 5# were shown in Fig. 3. The peak absorptions, maximum excitation and emission wavelengths centered at 274, 367 and 440 nm, respectively. The differences can be distinguished from the integrated and normalized UV–vis, excitation and emission spectra (see Fig. S2). With the organic solvent content in solution being increased, the absorption between 290 and 310 nm gradually red-shifted. Meanwhile, the maximum emission gradually broadened from sharp peak centered at 430 nm to broad one at 430–450 nm, but the maximum excitation, blue-shifted at band from 318 to 330 nm. Under the excitation of a 365 nm UV lamp, all the five C-dots can emit brightly blue light (see insets in Fig. 3A–E), suggesting the high QY of the C-dots.

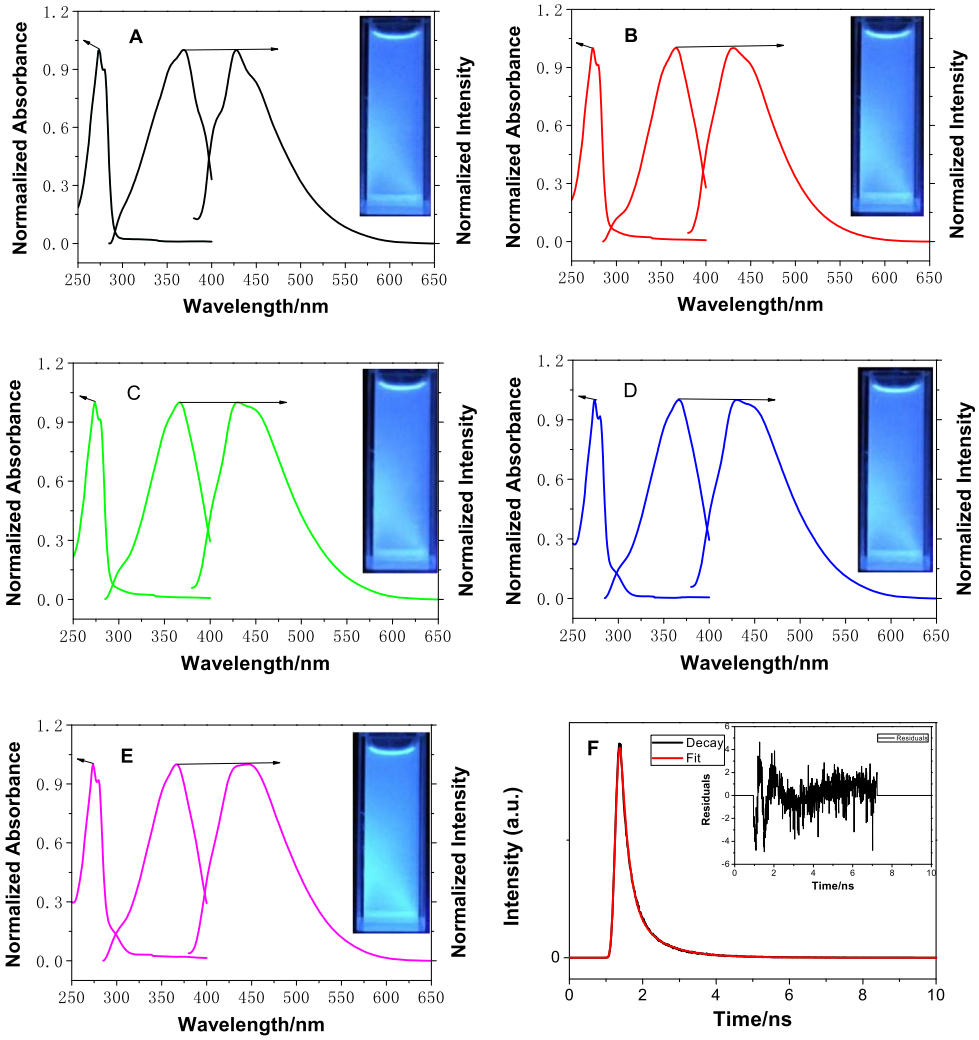

Fig. 3. Normalized UV–vis, excitation and emission spectra of 1# (A), 2# (B), 3# (C), 4# (D) and 5# (E) C-dots. Insets in A–E are the respective photographs taken under 365 nm UV lamp. Fluorescence decay for 5# C-dots in aqueous solution (F). Inset in F is the residual error.

The excitation-dependent emission is a common phenomenon for carbon-based fluorescent nanomaterials [19,29]. This phenomenon allows for multiple colors emitted *via* photoluminescence under different excitation wavelengths, which is of great significance for two-photonisc imaging and biomedical applications due to the effective avoidance of harmful UV or blue excitations [51]. When the excitation wavelengths were changed from 300 to 410 nm with an interval of 10 nm, the corresponding emission wavelengths for five C-dots all gradually red-shifted from 420 to 520 nm. Meanwhile, the emissions firstly enhanced, and then gradually decreased with the feature of 360 nm as a common maximum excitation wavelength (see Fig. S3). In addition, the spectra profiles seem very messy for 1# and 2# C-dots, but regular for other three ones. The QYs of the C-dots were also determined by slope method using quinine sulfate as a reference. From 1# to 5#, the QY value gradually increased from 15.3%, 16.5%, 16.8%, 18.6% to 19.6% (see Fig. S4), which are relatively great values among C-dots and suggests the tremendous potential of our C-dots for bioimaging.

Seeing that high QY of 5# C-dots, the pH- and time-dependent emissions, and effects of different solvents and ionic strength on emission were therefore further investigated. The C-dots is freely and easily dispersible in water, exhibiting good water solubility. The effect of time on emissions shown in Fig. S5A under UV irradiation indicates that the C-dots is highly resistant to photobleaching. Moreover, the emission behavior is independent of ionic strength of the medium. The emission almost remains unchanged with varied concentrations of NaCl in the aqueous solution (Fig. S5B). As shown in Fig. S6C, the emission enhanced with the increase of pH from 3 to 11. The presence of many —OH and a little COO^- group in the C-dots may have caused this relationship [16,52]. These groups make the C-dots similar to properties of amino acids, which are ampholytes and have varying isoelectric points and dissociation constants. This pH-dependent emission is further supported by zeta potential analysis (Fig. 2C).

The emission redshift for the C-dots is somewhat dependent on solvent as comparing DMF, THF, water and acetone (Fig. S7). This solvent effect could be caused by solvent attachment or the formation of different emissive traps on the surfaces of the C-dots [53,54]. The time-resolved fluorescence decay curve measured by the time-correlated single photon counting method is shown in Fig. 3F. The decay curve fits well to bi-exponent nature as demonstrated by the residuals. The fluorescence lifetime of the C-dots are $\tau_1 = 1.12$ ns and $\tau_2 = 4.49$ ns, and mean lifetime is calculated to be 1.74 ns. As shown in Fig. 3A–E, the PL peak at 440 nm can be excited in a narrow wavelength range. The main PL excitation

bands well agree with the corresponding defect-state absorption bands, suggesting that the emission is characterized by defect-state decay rather than bandedge exciton-state decay. This intrinsic PL characteristic is also exhibited in the PL decay curve, which shows di-exponential decay and one short lifetime [45].

3.1.3. The effect of temperature on preparation of insecticide-based C-dots

Temperature plays a key role in the synthesis of C-dots, which exerts great effect on QY, emission, morphology, and so on. The effects of temperature on the insecticide-based C-dots were also considered in the present work. Similar to the excitation-dependent emissions of solvothermal C-dots, when the carbonization temperature was increased from 150 to 170 °C, and the excitation wavelengths were changed from 300 to 400/410 nm with an interval of 10 nm, the corresponding emission wavelengths all gradually red-shifted from 420 to 520 nm. Meanwhile, the emissions took on first enhancement, and then gradual decrease featuring 360 nm as a common maximum excitation wavelength (see Fig. S8). In addition, the spectra profiles seem considerably messy for C-dots obtained at 150 and 160 °C. As shown Fig. 4A–C, different from the slight effect of solvent constitution on the spectra profiles, the peak absorption, maximum excitation and emission wavelength retain unchanged and centered at 273, 365 and 430 nm, respectively, at 150, 160 and 170 °C of carbonization temperature (see Fig. S9). The QYs of the C-dots were also determined as 5.3%, 11.36% and 19.6% for C-dots carbonized at 150, 160 and 170 °C (5# C-dots), respectively (see Fig. 4D), which agreed well with the images under 365 nm UV lamp (see insets in Fig. 3A–C). The effect of pH on emission of C-dots carbonized at 150 and 160 °C took on the same enhancement as that done at 170 °C (see Fig. S6A and B). The TEM results indicate that, different from the character of small size distribution and monodispersion of 5# C-dots, C-dots carbonized at relatively much lower temperature displayed much more irregular morphology and aggregation state (see Fig. S10). Therefore, properly high carbonized temperature and mixed solution with high organic content will be helpful to synthesize the eligible C-dots using 3-BP as a precursor.

3.2. Possible mechanisms and incompact framework structure of insecticide-based C-dots

It is now very difficult to propose definitive mechanisms for the preparation of C-dots owing to the harsh synthetic conditions and complicated carbonization of precursors, which does not, however, hamper us to infer some possible reactions according to the experimental results and concrete precursors [50,55]. Herein a possible mechanism as shown in Fig. 5 was proposed for the synthesis of insecticide-based C-dots. Two possible main classes of reaction happened among 3-BP molecules: one is a dehydrobromide to form phenyl ether analogue (denoted as Reaction 1). The other is a Yamamoto reaction to link aromatic rings through two Csp2 C—H direct binding (denoted as Reaction 2). Large number of Reactions 1 and 2 simultaneously arose to form polymer-like C-dots and finally carbogenic C-dots are formed by probable nuclear burst at supersaturation point. Providing essential evidences to confirm the mechanisms is required. Reaction 1 is a routine one to prepare phenyl ether, which was verified by the occurrence of C—O—C characteristic on FTIR spectrum (see Fig. 2A) [50]. The existence of Br^- on XPS spectrum also gave same result (see Fig. 1C). The ^{13}C NMR spectrum of C-dots with assignment of the resonances is shown in Fig. S11. The complex spectrum curve indicates the aromatic carbon was involved in complex chemical reaction. The signal peak at 132.6 ppm corresponds to the substituted phenyl carbons binding with oxygen atom. The signal peak at 98.2 possibly attributes to carbon binding with bromine atom due to shield effect. The signal peak for unsubstituted phenyl carbons is located at 117.7 ppm. The high-intensity peak at 124.5 ppm is ascribed to the signal peak of substituted phenyl carbons through Yamamoto reaction [47,48,56,57]. The strong Csp2 C—C peak on XPS spectrum,

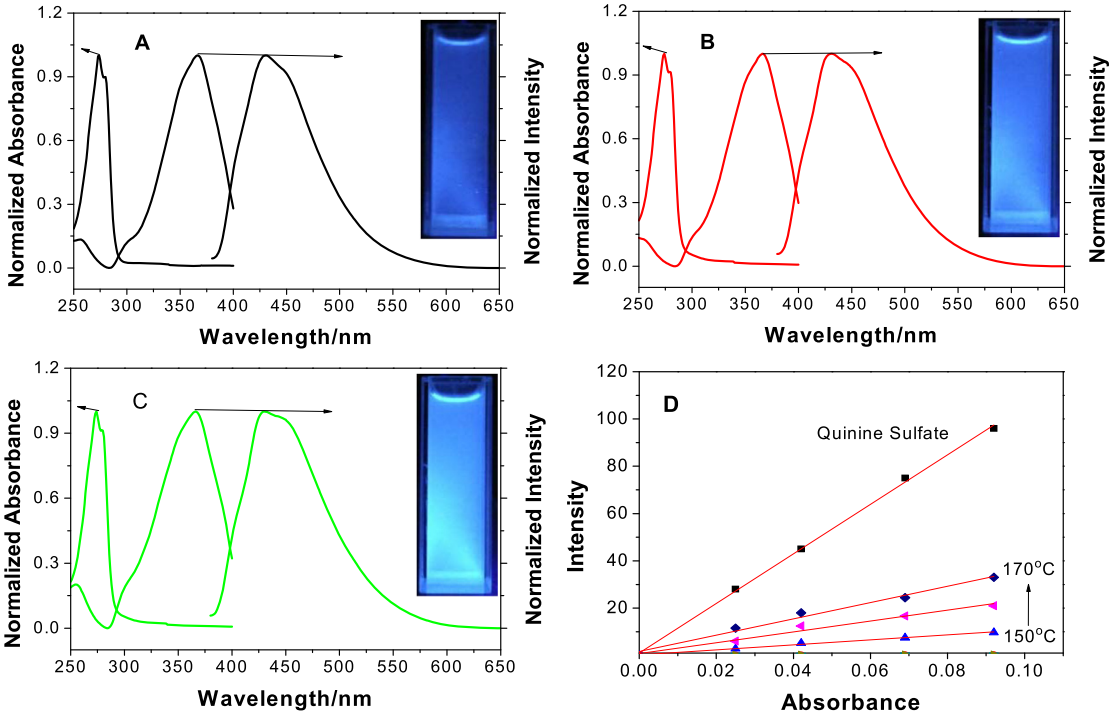

Fig. 4. Normalized UV–vis, excitation and emission spectra of C-dots carbonized at 150 °C (A), 160 °C (B) and 170 °C (C) in mixed solvent of ethanol and water (v/v, 9:1), respectively. Insets in A–C are the respective photographs taken under 365 nm UV lamp. Quantum yield calculation of C-dots carbonized at different temperature using quinine sulfate as a reference (D).

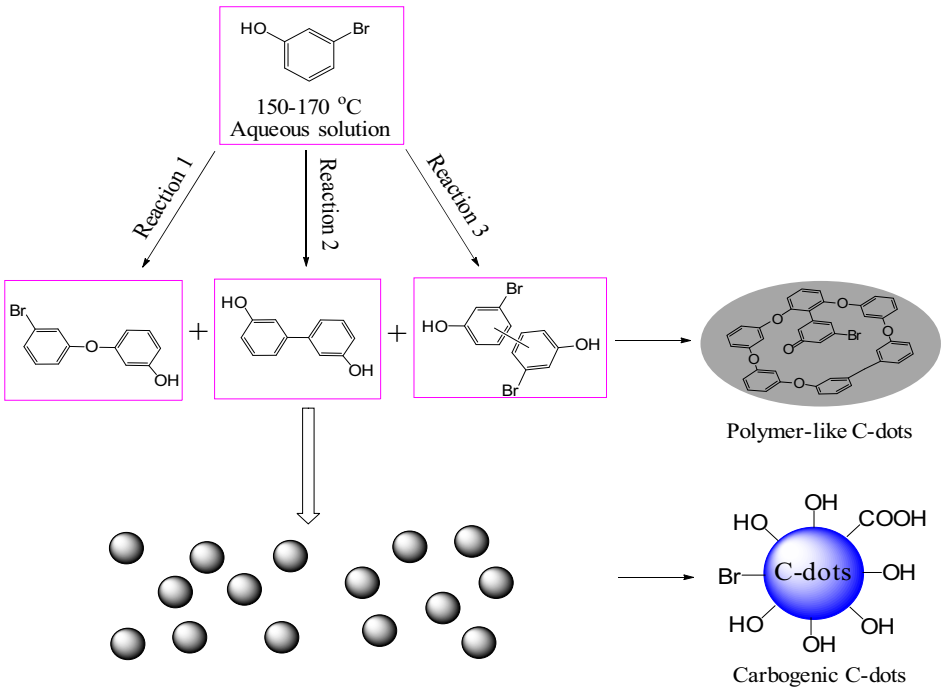

Fig. 5. Proposed possible mechanisms for the formation of insecticide-based C-dots.

to a certain extent, testified the existence of Yamamoto reaction. Friedel–Crafts reaction is another possible one to link two aromatic rings (denoted as Reaction 3). The strong Csp3 C—C peak on ^{13}C NMR spectrum demonstrates the possible occurrence of Friedel–Crafts reaction to link aromatic ring-containing molecules to form polymers (see Fig. S11) [58].

Because transition metal and rare-earth ions are deeply rooted in the host lattice of doped QDs and upconversion nanoparticles, respectively, the dissolved oxygen in solution is prevented from contacting with the excited triplet state, resulting in the effective phosphorescence [59,60]. Both FTIR and XPS spectra signal triplet-producing aromatic ring and triplet-promoting bromine in insecticide-based C-dots. Given the framework structure of our C-dots is as compact as that of doped QDs and upconversion nanoparticles, the triplet state will be activated and surprisingly efficient RTP will be therefore observed in both solid state and liquid state. As shown in Fig. S12, both the fluorescence and RTP at 528 nm with 3.7 ms of lifetime decay were observed in solid state at the same time, which testified the bromobenzene form still holds emission property of RTP. However, the RTP disappeared in liquid state, indicating the incompact framework structure of C-dots. This result will provide an innovative method for the determination of compactness of host materials.

3.3. Patterns printing using C-dots prepared by mimetic insecticide residuals as a colorless ink

To further verify the availability and practicability of the proposed method, a lab-leveled mimetic insecticide residuals approach was conducted to synthesize C-dots in the present work (see Fig. 6-left). In brief, 3-BP emulsion was sprayed on the surface of fruits and then dried prior to either wash the surface with ethanol or sonicate in water for 5 min. The resultant solution was collected, concentrated, excluded dissolved oxygen, and then transferred to the Teflon-lined autoclave and heated to 170 °C for 8 h. After naturally cooling to room temperature, the as-prepared C-dots was centrifuged at 10,000 rpm for 10 min to remove large precipitates. To further purify the C-dots, the concentrated C-dots were re-dispersed in mixed solution of 2:1 (v/v) water and dichloromethane for 3 times to remove the unreacted 3-BP molecules.

The highly bright C-dots was utilized as a colorless ink for printing patterns [47,55]. Colorless C-dots aqueous solution with concentration over 2.0×10^{-3} mg mL^{-1} was poured into a vacant cartridge from a commercial inkjet printer. This concentration is a critical one, which gave strong enough fluorescence to be detected under a UV lamp, making words and images visible. The original versions of Logo, Chinese/English names, School motto, and Entrance door with Hui Style of Anhui Jianzhu University (from up to bottom) are shown in Fig. S13. The printed versions were invisible in daylight, but were clearly observed under a hand-held 365 nm UV lamp (see Fig. 6-right). Moreover, the printed patterns retained their stability after it was placed among book pages for months, which is beneficial for practical applications.

3.4. Cytotoxicity and bioimaging of insecticide-based C-dots

The cytotoxicities of insecticide-based C-dots and 3-BP were evaluated using HeLa cells with an MTT viability assay. The concentration-dependent cell viabilities on C-dots and 3-BP are shown in Fig. 7A. At concentrations of 12.5, 25, 50 and 100 mg L^{-1}, the relative cell viability was about 85% for C-dots and 25% for 3-BP after a 48 h exposure even with a concentration of 100 mg L^{-1}. The results indicate insecticide-based C-dots not only show a low toxicity to the HeLa cells but also a much lower toxicity to the HeLa cells than 3-BP at relatively high concentration. Since the inherent toxicity of the C-dots is negligible, they could be used for potential biological applications such as bioimaging, protein analysis, cell tracking, isolation of biomolecules, and gene technology.

Bestowed with superior optical properties such as high QY, excellent photostability, low toxicity, good biocompatibility and high water solubility, the insecticide-based C-dots is expected to serve as excellent fluorescent probes for *in vitro* bioimaging. To evaluate this capability, HeLa cells were cultured in a culture medium, and confocal microscopic images were taken using a 405-nm laser at a low voltage. It can be seen from Fig. 7B–D that after incu-

Fig. 6. A lab-leveled mimetic insecticide residuals method to synthesize C-dots as colorless inks (left). Printed patterns obtained by C-dots ink and imaging under 365 nm UV lamp.

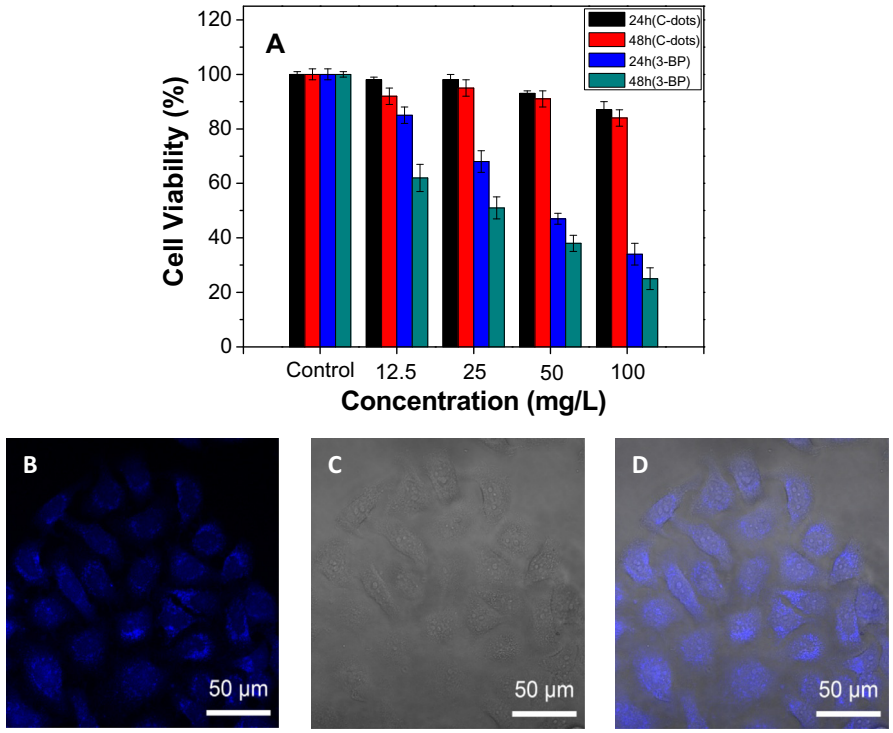

Fig. 7. Cellular toxicity and cellular imaging of C-dots. Effect of C-dots and 3-BP on HeLa cells viability (A), (B–D) are washed cells imaged underconfocal fluorescent (B), bright field (C), overlap of corresponding bright field image and fluorescence image (D).

bation of insecticide-based C-dots with HeLa cells, the blue emissions of C-dots sample could be clearly observed from HeLa cells when excited at 405 nm. The emissions mainly located at the areas of the cell membrane and cytoplasm, especially around the cell nucleus. Whereas the brightness of C-dots was very weak inside the cell nucleus [16,29,61]. Importantly, no morphological damage of the cells was observed upon incubation with C-dots further demonstrated their low cytotoxicity, indicating the insecticide-based C-dots have great potentials in bioimaging and other biomedical applications.

4. Conclusions

In summary, using 3-BP residual as a precursor to prepare C-dots was proven to be an effective strategy and an innovative method of making poison profitable. Higher organic solvent content in solution at same carbonization temperature resulted in a higher output of C-dots with analogue size and QY. Meanwhile, higher carbonization temperature using a same solution with high organic solvent content is in favor of the formation of C-dots with higher QY and smaller size. Interestingly, all insecticide-based C-

dots were completely water-soluble and remarkably stable against ionic strengths and light illumination. A lab-leveled mimetic insecticide residuals approach was adopted to synthesize C-dots at 170 °C and mixed solution of some (v/v) 9:1 of ethanol and water. They were utilized not only as colorless inks for printing patterns but also as fluorescence probe for bioimaging. Other pesticide and hazardous chemicals as precursors to prepare C-dots are in progress.

Acknowledgements

This work was supported by the Natural Science Foundation of China (21506002, 21301004, 21171004), and Natural Science Foundation of Anhui Province (1408085MB27, 1308085MB29), and Postdoctor Foundation (2013M530301) for financial support. The authors also thank the Doctor Foundation (2016) of Anhui Jianzhu University.

Appendix A. Supplementary data

Supplementary data associated with this article can be found, in the online version, at http://dx.doi.org/10.1016/j.cej.2016.03.004.

References

[1] Y.P. Sun, B. Zhou, Y. Lin, W. Wang, K.A.S. Fernando, P. Pathak, M.J. Meziani, B.A. Harruff, X. Wang, H. Wang, Quantum-sized carbon dots for bright and colorful photoluminescence, J. Am. Chem. Soc. 128 (2006) 7756–7757.
[2] L. Zheng, Y. Chi, Y. Dong, J. Lin, B. Wang, Electrochemiluminescence of water-soluble carbon nanocrystals released electrochemically from graphite, J. Am. Chem. Soc. 131 (2009) 4564–4565.
[3] S.N. Baker, G.A. Baker, Luminescent carbon nanodots: emergent nanolights, Angew. Chem. Int. Ed. 122 (2010) 6876–6896.
[4] X.T. Zheng, A. Ananthanarayanan, K.Q. Luo, P. Chen, Glowing graphene quantum dots and carbon dots: properties, syntheses, and biological applications, Small 11 (2015) 1620–1636.
[5] L. Li, G. Wu, G. Yang, J. Peng, J. Zhao, J.J. Zhu, Focusing on luminescent graphene quantum dots: current status and future perspectives, Nanoscale 5 (2013) 4015–4039.
[6] A. Zhao, Z. Chen, C. Zhao, N. Gao, J. Ren, X. Qu, Recent advances in bioapplications of C-dots, Carbon 85 (2015) 309–327.
[7] X. Michalet, F.F. Pinaud, L.A. Bentolila, J.M. Tsay, S. Doose, J.J. Li, G. Sundaresan, A.M. Wu, S.S. Gambhir, S. Weiss, Quantum dots for live cells, in vivo imaging, and diagnostics, Science 307 (2005) 538–544.
[8] K. Sanderson, Quantum dots go large, Nature 459 (2009) 760–761.
[9] J. Jung, A. Solanki, K.A. Memoli, K. Kamei, H. Kim, M.A. Drahl, Selective inhibition of human brain tumor cells through multifunctional quantum-dot-based siRNA delivery, Angew. Chem. Int. Ed. 49 (2010) 103–107.
[10] H.T. Li, X.D. He, Y. Liu, H. Huang, S.Y. Lian, S.T. Lee, Z. Kang, One-step ultrasonic synthesis of water-soluble carbon nanoparticles with excellent photoluminescent properties, Carbon 49 (2011) 605–609.
[11] L. Cao, X. Wang, M.J. Meziani, F. Lu, H. Wang, P.G. Luo, Carbon dots for multiphoton bioimaging, J. Am. Chem. Soc. 129 (2007) 11318–11319.
[12] O. Stephan, P.M. Ajayan, C. Colliex, P. Redlich, J.M. Lambet, P. Bernier, Doping graphitic and carbon nanotube structures with boron and nitrogen, Science 266 (1994) 1683–1685.
[13] B.B. Bourlinos, A. Bakandritsos, A. Kouloumpis, D. Gournis, M. Krysmann, E.P. Giannelis, K. Polakova, K. Safarova, K. Hola, R. Zboril, Gd(III)-doped carbon dots as a dual fluorescent-MRI probe, J. Mater. Chem. 22 (2012) 23327–23330.
[14] S. Liu, J.Q. Tian, L. Wang, Y.W. Zhang, X.Y. Qin, Y.L. Luo, A.M. Asiri, A.O. Al-Youbi, X. Sun, Hydrothermal treatment of grass: a low-cost, green route to nitrogen-doped, carbon-rich, photoluminescent polymer nanodots as an effective fluorescent sensing platform for label-free detection of Cu(II) ions, Adv. Mater. 24 (2012) 2037–2041.
[15] F. Wang, Z. Xie, H. Zhang, C.Y. Liu, Y.G. Zhang, Highly luminescent organosilane-functionalized carbon dots, Adv. Funct. Mater. 21 (2011) 1027–1031.
[16] Y.Q. Zhang, D.K. Ma, Y. Zhuang, X. Zhang, W. Chen, L.L. Hong, Q.X. Yan, K. Yu, S. M. Huang, One-pot synthesis of N-doped carbon dots with tunable luminescence properties, J. Mater. Chem. 22 (2012) 16714–16718.
[17] D. Sun, R. Ban, P.H. Zhang, G.H. Wu, J.R. Zhang, J.J. Zhu, Hair fiber as a precursor for synthesizing of sulfur- and nitrogen-co-doped carbon dots with tunable luminescence properties, Carbon 64 (2013) 424–434.
[18] Y. Dong, L. Wan, J. Cai, Q. Fang, Y. Chi, G. Chen, Natural carbon-based dots from humic substances, Sci. Rep. 5 (2015), http://dx.doi.org/10.1038/srep10037.
[19] Y. Dong, C. Chen, X. Zheng, L. Gao, Z. Cui, H. Yang, C. Guo, Y. Chi, C.M. Li, One-step and high yield simultaneous preparation of single- and multi-layer graphene quantum dots from CX-72 carbon black, J. Mater. Chem. 22 (2012) 8764–8766.
[20] L. Wang, H.S. Zhou, Green synthesis of luminescent nitrogen-doped carbon dots from milk and its imaging application, Anal. Chem. 86 (2014) 8902–8905.
[21] S. Jahan, F. Mansoor, S. Naz, J. Lei, S. Kanwal, Oxidative synthesis of highly fluorescent boron/nitrogen co-doped carbon nanodots enabling detection of photosensitizer and carcinogenic dye, Anal. Chem. 85 (2013) 10232–10239.
[22] H. Peng, J. Travas-Sejdic, Simple aqueous solution route to luminescent carbogenic dots from carbohydrates, Chem. Mater. 21 (2009) 5563–5565.
[23] H. Zhu, X. Wang, Y. Li, Z. Wang, F. Yang, X. Yang, Microwave synthesis of fluorescent carbon nanoparticles with electrochemiluminescence properties, Chem. Commun. 5118–5120 (2009).
[24] R. Liu, D. Wu, S. Liu, K. Koynov, W. Knoll, Q. Li, An aqueous route to multicolor photoluminescent carbon dots using silica spheres as carriers, Angew. Chem. Int. Ed. 121 (2009) 4598–4601.
[25] C.W. Lai, Y.H. Hsiao, Y.K. Peng, P.T. Chou, Facile synthesis of highly emissive carbon dots from pyrolysis of glycerol: gram scale production of carbon dots/mSiO(2) for cell imaging and drug release, J. Mater. Chem. 22 (2012) 14403–14409.
[26] H. Liu, T. Ye, C. Mao, Fluorescent carbon nanoparticles derived from candle soot, Angew. Chem. Int. Ed. 46 (2007) 6473–6475.
[27] H. Huang, J.J. Lv, D.L. Zhou, N. Bao, Y. Xu, A.J. Wang, One-pot green synthesis of nitrogen-doped carbon nanoparticles as fluorescent probes for mercury ions, RSC Adv. 3 (2013) 691–696.
[28] H. Huang, Y. Xu, C.J. Tang, J.R. Chen, A.J. Wang, J.J. Feng, Facile and green synthesis of photoluminescent carbon nanoparticles for cellular imaging, New J. Chem. 38 (2014) 784–789.
[29] S. Sahu, B. Behera, T.K. Maiti, S. Mohapatra, Simple one-step synthesis of highly luminescent carbon dots from orange juice: application as excellent bio-imaging agents, Chem. Commun. 48 (2012) 8835–8837.
[30] C. Aranda, F. Godoy, J. Becerra, R. Barra, P. Martínez, Aerobic secondary utilization of a non-growth and inhibitory substrate 2,4,6-trichlorophenol by *Sphingopyxis chilensis* S37 and *Sphingopyxis*-like strain S32, Biodegradation 14 (2003) 265–274.
[31] L. Xun, C. Webster, A monooxygenase catalyzes sequential dechlorinations of 2,4,6-trichlorophenol by oxidative and hydrolytic reactions, J. Biol. Chem. 279 (2004) 6696–6700.
[32] M. Gutiérrez, J. Becerra, R. Barra, Tribromophenol empleado en aserraderos: métodos de análisis, características físico-químicas y presencia en componentes ambientales, Bol. Soc. Chil. Quim. 47 (2002) 485–493.
[33] T. Hassenklöver, S. Predehl, J. Pilli, J. Ledwolorz, M. Assmann, U. Bickmeyer, Bromophenols, both present in marine organisms and industrial flame retardants, disturb cellular Ca^{2+} signaling in neuroendocrine cells (PC12), Aquat. Toxicol. 76 (2006) 37–45.
[34] I. Legler, A. Brouwer, Are brominated flame retardants endocrine disruptors?, Environ Int. 29 (2003) 879–885.
[35] C.M. Olsen, E.T.M. Meussen-Elholm, J.A. Holme, J.K. Hongslo, Brominated phenols: characterization of estrogen-like activity in the human breast cancer cell-line MCF-7, Toxicol. Lett. 129 (2002) 55–63.
[36] P. Beltrame, P.L. Beltrame, P. Carniti, D. Guardione, C. Lanzetta, Inhibiting action of chlorophenols on biodegradation of phenol ant its correlations with structural properties of inhibitors, Biotechnol. Bioeng. 31 (1988) 821–828.
[37] S.Y. Dapaah, G.A. Hill, Biodegradation of chlorophenol mixtures by *Pseudomonas putida*, Biotechnol. Bioeng. 40 (1992) 1353–1358.
[38] H.A. Sharma, J.T. Berber, H.E. Ensley, M.A. Polito, A comparison of the toxicity and metabolism of phenol and chlorinated phenols by *Lemma gibba*, with special reference to 2,4,5-trichlorophenol, Environ. Toxicol. Chem. 16 (1997) 346–350.
[39] K. Arnoldsson, P.L. Andersson, P. Haglund, Formation of environmentally relevant brominated dioxins from 2,4,6,-tribromophenol via bromoperoxidase-catalyzed dimerization, Environ. Sci. Technol. 46 (2012) 7239–7244.
[40] J. Yang, S. Cui, J.Q. Qiao, H.Z. Lian, The photocatalytic dehalogenation of chlorophenols and bromophenols by cobalt doped nano TiO_2, J. Mol. Catal. A Chem. 395 (2014) 42–51.
[41] H. Zheng, Q. Wang, Y. Long, H. Zhang, X. Huang, R. Zhu, Enhancing the luminescence of carbon dots with a reduction pathway, Chem. Commun. 47 (2011) 10650–10652.
[42] P. Shen, Y. Xia, Synthesis–modification integration: one-step fabrication of boronic acid functionalized carbon dots for fluorescent blood sugar sensing, Anal. Chem. 86 (2014) 5323–5329.
[43] S.H. Liu, F. Lu, X.D. Jia, F.F. Cheng, L.P. Jiang, J.J. Zhu, Microwave assisted synthesis of a biocompatible polyacid conjugated Fe_3O_4 superparamagnetic hybrid, CrystEngComm 13 (2011) 2425–2429.
[44] P. Vijayan, C. Mahendiran, C. Suresh, K. Shanthi, Photocatalytic activity of iron doped nanocrystalline titania for the oxidative degradation of 2,4,6-trichlorophenol, Catal. Today 141 (2009) 220–224.
[45] L. Wang, Y. Wang, T. Xu, H. Liao, C. Yao, Y. Liu, Z. Li, Z. Chen, D. Pan, L. Sun, M. Wu, Gram-scale synthesis of single-crystalline grapheme quantum dots with superior optical properties, Nat. Commun. 5 (2014), http://dx.doi.org/10.1038/ncomms6357.
[46] Z. Zhang, Y. Shi, Y. Pan, X. Cheng, L. Zhang, J. Chen, M.J. Li, C. Yi, Quinoline derivative-functionalized carbon dots as a fluorescent nanosensor for sensing and intracellular imaging of Zn^{2+}, J. Mater. Chem. B 2 (2014) 5020–5027.
[47] S. Zhu, Q. Meng, L. Wang, J. Zhang, Y. Song, H. Jin, K. Zhang, H. Sun, H. Wang, B. Yang, Highly photoluminescent carbon dots for multicolor patterning, sensors, and bioimaging, Angew. Chem. Int. Ed. 125 (2013) 3953–3957.

[48] E. Papirer, R. Lacroix, J.B. Donnet, G. Nanse, P. Froux, XPS study of the halogenation of carbon black-part 1. Bromonation, Carbon 32 (1994) 1341–1358.
[49] V. Chandra, J. Park, Y. Chun, J.W. Lee, I.C. Hwang, K.S. Kim, Water-dispersible magnetite-reduced graphene oxide composites for arsenic removal, ACS Nano 4 (2010) 3979–3986.
[50] Y. Li, H. Zhang, P. Liu, D. Wang, Y. Li, H. Zhao, Cross-linked g-C_3N_4/rGO nanocomposites with tunable band structure and enhanced visible light photocatalytic activity, Small 9 (2013) 3336–3344.
[51] S.J. Zhu, J.H. Zhang, S.J. Tang, C.Y. Qiao, L. Wang, H.Y. Wang, X. Liu, B. Li, Y. Li, W. Yu, Surface chemistry routes to modulate the photoluminescence of graphene quantum dots: from fluorescence mechanism to up-conversion bioimaging applications, Adv. Funct. Mater. 22 (2012) 4732–4740.
[52] J. Jiang, Y. He, S.Y. Li, H. Cui, Amino acids as the source for producing carbon nanodots: microwave assisted one-step synthesis, intrinsic photoluminescence property and intense chemiluminescence enhancement, Chem. Commun. 48 (2012) 9634–9636.
[53] J.P. Paraknowitsch, Y.J. Zhang, B. Wienert, A. Thomas, Nitrogen and phosphorus-co-doped carbons with tunable enhanced surface areas promoted by the doping additives, Chem. Commun. 49 (2013) 1208–1210.
[54] D.Y. Pan, J.C. Zhang, Z. Li, C. Wu, X.M. Yan, M.H. Wu, Observation of pH-, solvent-, spin-, and excitation-dependent blue photoluminescence from carbon nanoparticles, Chem. Commun. 46 (2010) 3681–3683.
[55] X. Chen, Q. Jin, L. Wu, C. Tung, X. Tang, Synthesis and unique photoluminescence properties of nitrogen-rich quantum dots and their applications, Angew. Chem. Int. Ed. 53 (2014) 12542–12547.
[56] L. Zhou, X. Zhang, Q. Wang, Y. Lv, G. Mao, A. Luo, Y. Wu, Y. Wu, J. Zhang, W. Tan, Molecular engineering of a TBET-based two-photon fluorescent probe for ratiometric imaging of living cells and tissues, J. Am. Chem. Soc. 136 (2014) 9838–9841.
[57] Q. Chen, M. Luo, P. Hammershøj, D. Zhou, Y. Han, B.W. Laursen, C.G. Yan, B.H. Han, Microporous olycarbazole with high specific surface area for gas storage and separation, J. Am. Chem. Soc. 134 (2012) 6084–6087.
[58] R. Dawson, L.A. Stevens, T.C. Drage, C.E. Snape, M.W. Smith, D.J. Adams, A.I. Cooper, Impact of water coadsorption for carbon dioxide capture in microporous polymer sorbents, J. Am. Chem. Soc. 134 (2012) 10741–10744.
[59] W.S. Zou, D. Sheng, X. Ge, J.Q. Qiao, H.Z. Lian, Room-temperature phosphorescence (RTP) chemosensor and Rayleigh scattering (RS) chemodosimeter dual-recognition probe for 2,4,6-trinitrotulene based on Mn-doped ZnS quantum dots, Anal. Chem. 83 (2011) 30–37.
[60] W.S. Zou, J.Q. Qiao, X. Hu, X. Ge, H.Z. Lian, Synthesis in aqueous solution and characterization of a new cobalt doped ZnS quantum dots as a hybrid ratiometric chemoensor, Anal. Chim. Acta 708 (2011) 134–140.
[61] V. Gupta, N. Chaudhary, R. Srivastava, G.D. Sharma, R. Bhardwaj, S. Chand, Luminscent graphene quantum dots for organic photovoltaic devices, J. Am. Chem. Soc. 133 (2011) 9960–9963.